23rd ABCM International Congress of Mechanical Engineering
December 6-11, 2015, Rio de Janeiro, RJ, Brazil

STEADY FLAMELET MODELING OF A NON-PREMIXED TURBULENT $CH_4/H_2/N_2$-AIR FLAME WITH AND WITHOUT RADIATION

Diego Luis Deon[*]
Fernando Marcelo Pereira[†]
UFRGS - Federal University of Rio Grande do Sul, Mechanical Engineering Department, Porto Alegre, RS, Brazil
[*] diego_dld@hotmail.com, [†] fernando@mecanica.ufrgs.br

Abstract. *A non-premixed turbulent $CH_4/H_2/N_2$ flame, surrounded by a low-velocity air coflow, is numerically reproduced employing the steady laminar flamelet concept. In this technique, the mean reactive scalars, i.e., temperature and species mass fractions, are obtained from the solution of quasi-unidimensional counter-flow flames, named flamelets. The results are stored in a databank, parameterized by mixture fraction, its variance and dissipation rate. To generate the flamelet library, the turbulence-chemistry interaction is taken into account through presumed probability density functions of these mean scalars. Thus, to solve the complete flow problem, there is no need to deal with the highly coupled energy and species partial differential equations, since their mean values are recovered from the flamelet library, reducing drastically the computational time required to achieve results convergence. The flame under investigation is widely exploited, being the target from several numerical approaches. The numerical results are compared to the experimental ones, in order to show the agreement level to measurements and the ones obtained by other researchers. The predicted quantities have shown to be in reasonable agreement with experimental data, for longitudinal velocity, mixture fraction, temperature and species mass fractions. However, some discrepancies exist, like in NO predictions, what is presumed to be due to some simplifications present in the model.*

Keywords: *steady laminar flamelet model, non-premixed flame, turbulent combustion, Flame DLR-A*

1. INTRODUCTION

Non-premixed flames, also referred to diffusion flames, are certainly the most frequently encountered flames in combustion systems, especially in industrial applications, due to safety reasons. And, despite the theoretical complexity of the turbulent combustion, the participation of turbulence in conjunction with chemical reactions is usually quite advantageous for practical purposes, since it benefits reactants mixing and heat transport, due to turbulent diffusion to be much higher than the molecular one.

Due to difficulties in the numerical simulation of such flames, they were studied almost exclusively empirically along many years. Significant theoretical advances in their understanding came only at the end of the 1970s, supported in part by the advance in computation (Law, 2006). However, the numerical simulation of turbulent flames is still a challenge to computational fluid dynamics, making the most complete and realistic numerical models almost forbidden even for scientific researches. This problem led to a series of approaches aiming at reducing the computational time.

One of these alternatives is based on the flamelet concept. The flamelet model assumes that a multidimensional turbulent flame can be seen as an ensemble of quasi-unidimensional laminar flame structures, named flamelets. This approach allows for the decoupling of the chemical reactions and the turbulent flow field (Peters, 1984 and 1986). Each flamelet is subjected to local flow field conditions, resulting in their convection and stretching. Therefore, the local flame structure can be described only by local flow parameters, usually the mixture fraction and its scalar dissipation rate. The laminar flamelet structure can be pre-calculated and tabulated into a flamelet library, a databank containing the main reactive scalars, parameterized by a few number of control variables. Once the values of these parameters are known from the flow field, one can find the thermo-chemical quantities from the flamelet library.

Further developments of this model made it a powerful tool and quite popular in the combustion community. The model has been successfully applied to predict flow variables in many applications, both for laminar and turbulent flames (Lentini and Puri, 1995; Sanders *et al.*, 1997; Pitsch, 2000; Coelho and Peters, 2001; Wen *et al.*, 2003; Claramunt, 2005; Hossain and Malalasekera, 2005; Yilmaz *et al.*, 2005; Odedra and Malalasekera, 2007; Lee and Choi, 2009; Ravikanti *et al.*, 2009; Emami and Fard, 2012; Ziani *et al.*, 2013).

Therefore, the problem under investigation in this work concerns the use of the steady flamelet modeling approach in a non-premixed turbulent flame of methane enriched with hydrogen and diluted with nitrogen, surrounded by a low-velocity air coflow, named Flame DLR-A, due to the laboratory which conducted it experimentally, the DLR Institute of Combustion Technology from Stuttgart (Bergmann, 1998). It has been widely exploited, being the target from several numerical approaches (Pitsch, 2000; Kim *et al.*, 2005; Yilmaz *et al.*, 2005; Tabet-Helal *et al.*, 2007; Lee and Choi, 2009; Klewer, 2011; Emami and Fard, 2012; Ziani *et al.*, 2013). Results are compared to those obtained by measurements and other numerical simulations.

2. PROBLEM CHARACTERIZATION

At the third International Workshop on Measurement and Computation of Turbulent Nonpremixed Flames, held in 1998, one of the target cases for the event was a non-premixed turbulent flame of a mixture of methane (CH_4), hydrogen (H_2) and nitrogen (N_2) surrounded by a low-velocity coflow of air (TNF Workshop, 1998). This flame has been proposed by the DLR Institute of Combustion Technology from Stuttgart (Bergmann, 1998), and was subsequently conducted experimentally by two other laboratories, the Sandia National Laboratory from Livermore (Meier *et al.*, 2000), and the Technisque Universität Darmstadt (Schneider *et al.*, 2003).

The fuel, a mixture of 22.1% CH_4, 33.2 H_2 and 44.7% N_2 (by volume), is supplied by a vertical stainless steel tube with internal diameter, *D*, equal to 8 mm, with a thinned rim at the exit, and a 350 mm long straight cross-section prior to exit. Its bulk velocity, 42.15 m/s, corresponds to a Reynolds number equal to 15,200 based on internal diameter of the pipe. Its stoichiometric mixture fraction, Z_{st}, is equal to 0.167 and the adiabatic flame temperature, T_{ad}, to 2,130 K.

The air stream, in turn, is provided by a forced-draft vertical wind tunnel, and has a velocity of 0.3 m/s. In the case of DLR Institute of Combustion Technology and Technisque Universität Darmstadt, dry air is discharged by a circular nozzle, with an internal diameter of 140 mm. In the case of Sandia National Laboratory experiments, air stream has 0.8% water vapor by volume and its outlet nozzle is square and 300 mm wide, with the fuel pipe centered on it. This difference between the air coflow suppliers, however, may not be significant, since its velocity is very low, being the room air the responsible for providing most of the oxidant needed by the flame.

Both streams of fuel and oxidant and the environment are maintained at the temperature of 292 K. Ambient pressure, in turn, is reported to be 95.3 kPa on DLR Institute of Combustion Technology, and 99.0 kPa in the case of Sandia National Laboratory, and no information is available for Technisque Universität Darmstadt.

Velocity measurements were conducted at the Technisque Universität Darmstadt, through the laser Doppler velocimetry (LDV) technique, providing the mean values for longitudinal and transversal velocities, with a reported statistical error below 5%. Temperature measurements, performed at Sandia National Laboratory, were obtained by Rayleigh scattering, for which the authors estimate an order of uncertainty of 3%. Also at Sandia National Laboratory were measured the mass fractions for eight chemical species (CH_4, N_2, O_2, CO_2, H_2O, H_2, OH and NO) obtained by Raman scattering, and one more, monoxide carbon (CO), obtained through the two-photon laser-induced fluorescence (LIF), technique which the authors assume to be more reliable for this species in particular. The order of the uncertainties estimated for the mass fractions of the species is varied, ranging from 3 up to 20%. From these nine species is also possible to calculate the mixture fraction. The experimental data are digitally available and can be accessed on Sandia National Laboratories website (Sandia National Laboratories).

In this work were adopted the original geometrical configuration and experimental conditions, i.e., as reported by DLR Institute of Combustion Technology.

3. NUMERICAL MODELING

3.1 Flow modeling

The flow problem was solved numerically employing Reynolds-Averaged Navier-Stokes (RANS) equations for conservation of total mass and momentum, assuming the Stokes hypothesis for a Newtonian fluid in steady-state,

$$\boldsymbol{\nabla} \cdot (\overline{\rho}\, \widetilde{\boldsymbol{u}}) = 0 \tag{1}$$

$$\boldsymbol{\nabla} \cdot (\overline{\rho}\, \widetilde{\boldsymbol{u}}\, \widetilde{\boldsymbol{u}}) = -\boldsymbol{\nabla}\tilde{p} + \boldsymbol{\nabla} \cdot \left[\mu \left(\boldsymbol{\nabla}\widetilde{\boldsymbol{u}} + (\boldsymbol{\nabla}\widetilde{\boldsymbol{u}})^T - \frac{2}{3}\boldsymbol{\nabla}\widetilde{\boldsymbol{u}}\, \boldsymbol{I}\right) - \overline{\rho}\, \widetilde{\boldsymbol{u}''\, \boldsymbol{u}''}\right] + \overline{\rho}\, \boldsymbol{g} \tag{2}$$

where $\boldsymbol{u}$ is the flow velocity vector, ρ is the mixture density, p is the system pressure, $\boldsymbol{g}$ is the gravity vector, μ is the dynamic molecular (or laminar) viscosity and $\boldsymbol{I}$ is the identity matrix.

All equations are written using mass-weighted averages, i.e., the Favre averages, where the tilde denotes the terms in which is applied the Favre average and the overbar denotes the terms in which is applied a simple temporal average, the Reynolds average.

In Eq. (2) the Reynolds stresses term is closed following the Boussinesq hypothesis, i.e., assuming that the turbulent stresses can be treated in an analogous way to the stresses in laminar flows (Wilcox, 1998),

$$-\overline{\rho}\, \widetilde{\boldsymbol{u}''\, \boldsymbol{u}''} = \mu_t[\boldsymbol{\nabla}\widetilde{\boldsymbol{u}} + (\boldsymbol{\nabla}\widetilde{\boldsymbol{u}})^T] - \frac{2}{3}\overline{\rho}\, \tilde{k}\, \boldsymbol{I} \tag{3}$$

where μ_t is the turbulent (or eddy) dynamic viscosity and k is the turbulence kinetic energy.

Modeling k and μ_t is a task which depends on the turbulence closure model. In this study was employed the Standard k-ε model, proposed by Launder and Spalding (1972), with a modified value for constant $C_{\varepsilon 1}$, which controls

the generation of the turbulent kinetic energy dissipation rate, from 1.44 to 1.60, according to proposal made by Morse (1977) and Pope (1978). This modification is quite popular and aims to correct an over-estimation on the decay rate of the turbulent kinetic energy on the Standard *k-ε* model (Dally *et al.*, 1998), and has shown to overcome shortcomings in the prediction of free round jets, with or without combustion (Pitsch, 2000; Smith *et al.*, 2003; Smith *et al.*, 2004; Emami and Fard, 2012; Zakrzewski and Ziolkowski, 2013; Ziani *et al.*, 2013; Deon *et al.*, 2014).

3.2 Steady laminar diffusion flamelet model

In non-premixed flames, combustion takes place in a thin layer in the vicinity of the surface of the stoichiometric mixture fraction. In general, non-premixed combustion is associated to diffusive flamelets in counter-flow configuration, in which fuel and oxidant are injected one against the other through opposed axisymmetric nozzles. As the distance between the nozzles is decreased or increased the flow rate of the jets, the flame is deformed in order to compress it longitudinally and stretch it in the transverse direction, distancing it from the chemical equilibrium condition, until it is completely extinguished.

The equations that describe the flamelet structure in a counter-flow configuration is based on the mixture fraction, Z. If assumed that its local gradient is sufficiently high, and under certain simplifying assumptions, can be said that the fluid thermo-chemical state is related to it (Peters, 1984 and 1986). There are several alternatives for formulating the mixture fraction, depending on the fuel composition and the characteristics of the phenomenon that are aimed to be captured. Nevertheless, whatever the definition, it should follow the premise of being equal to 0 in the oxidizer stream and to 1 in the fuel, and by presenting any monotonic behavior over the spatial resolution of the flamelet. For fuels composed by hydrocarbons it is usual to use the mixture fraction as defined by Bilger (1988),

$$Z = \frac{2\left(Y_C - Y_{C,2}\right)/W_C + 0.5\left(Y_H - Y_{H,2}\right)/W_H - \left(Y_O - Y_{O,2}\right)/W_O}{2\left(Y_{C,1} - Y_{C,2}\right)/W_C + 0.5\left(Y_{H,1} - Y_{H,2}\right)/W_H - \left(Y_{O,1} - Y_{O,2}\right)/W_O} \tag{4}$$

where Y_i and W_i are the mass fractions and atomic weights corresponding to atoms of carbon (C), hydrogen (H) and oxygen (O) present in the mixture. Sub-indices 1 and 2 refer to streams of pure fuel and oxidant, respectively.

In the steady laminar diffusion flamelet model species and energy equations are rewritten in the mixture fraction space, assuming unity Lewis number and using the Crocco-type coordinate transformation and a subsequent asymptotic analysis of the order of magnitude for individual terms, leading to

$$\frac{1}{2}\rho\,\chi\frac{\partial^2 Y_k}{\partial Z^2} + \dot{\omega}_k = 0 \quad for \quad k = 1, N_k - 1 \tag{5}$$

$$\frac{1}{2}\rho\,\chi\frac{\partial^2 T}{\partial Z^2} - \frac{1}{c_p}\sum_{k=1}^{N_k} h_k\,\dot{\omega}_k + \frac{1}{2}\frac{\rho\,\chi}{c_p}\left(\frac{\partial c_p}{\partial Z} + \sum_{k=1}^{N_k} c_{p,k}\frac{\partial Y_k}{\partial Z}\right)\frac{\partial T}{\partial Z} = 0 \tag{6}$$

where T is the temperature, χ is the scalar dissipation rate, Y_k is the mass fraction of a species k, $\dot{\omega}_k$ is its mass production rate, h_k is its specific enthalpy, and $c_{p,k}$ and c_p are the k^{th} species specific heat and the mixture-averaged specific heat, respectively.

The scalar dissipation rate, χ, is a parameter that quantifies the influence of multidimensional effects on the flow field. It has the dimension s^{-1}, and can be interpreted as a characteristic diffusion time of the flamelet. It is commonly obtained from asymptotic solutions. In this numerical code is employed the formulation from Kim and Williams (1997),

$$\chi = \frac{a_s}{4\,\pi}\frac{3\left(\sqrt{\rho_\infty/\rho}+1\right)^2}{2\sqrt{\rho_\infty/\rho}+1}\,exp\{-2[erfc^{-1}(2\,Z)]^2\} \tag{7}$$

where $erfc^{-1}$ is the inverse of complementary error function, ρ_∞ is the density of the oxidant stream and a_s is the characteristic strain rate of the flamelet, used as boundary condition for solving the flamelet equations,

$$a_s = 0.5\,V\,d^{-1} \tag{8}$$

where V is the relative velocity of the streams issuing from the fuel and oxidant jets and d is the distance between the jets nozzles. Thus, the scalar dissipation rate varies along the flamelet, and a characteristic value must be chosen to parameterize the results. In this study it is based on the position in which the mixture fraction is stoichiometric, χ_{st}.

Defined the appropriate conditions for the problem, i.e., the boundary conditions for temperature, pressure and species mass fractions at the streams output of fuel and oxidant, the flamelet equations are solved for a wide range of χ_{st}, that can be obtained by varying the strain rate parameter a_s, starting from low values, near the chemical

equilibrium condition, $\chi_{st} \to 0$, until the flame extinguishment. The solutions for species mass fractions and temperature are stored as functions of mixture fraction and stoichiometric scalar dissipation rate.

The influence of turbulent fluctuations on thermo-chemical quantities are taken into account by using a probability density function (PDF) and the beta-function distribution, first introduced on combustion literature by Janicka and Kollman (1979). Assuming statistical independence between the variables that comprise the PDF, can be computed the averaged values for temperature, mixture density and species mass fractions. These solutions are stored as functions of a few number of control variables, namely, the mean mixture fraction, $\tilde{Z}$, its variance, $\widetilde{Z''^2}$, the mean stoichiometric scalar dissipation rate, $\widetilde{\chi_{st}}$, and the mean system total enthalpy, $\tilde{H}$. The variances for χ_{st} and H are not needed because the effect of their fluctuations over the thermo-chemical quantities mean values is commonly assumed negligible.

The averaged scalar dissipation rate is obtained through an algebraic equation, which is related to fluctuations of mixture fraction variance and flow turbulence scales, as follows

$$\widetilde{\chi_{st}} = C_\chi \frac{\tilde{\varepsilon}}{\tilde{k}} \widetilde{Z''^2} \tag{9}$$

where C_χ is a constant, equal to 2.

The system total enthalpy, $\tilde{H}$, in turn, is determined by a simplified expression for the balance of energy, as follows

$$\boldsymbol{\nabla} \cdot \left(\overline{\rho}\, \tilde{\boldsymbol{u}}\, \tilde{H}\right) = \boldsymbol{\nabla} \cdot \left(\frac{k_t}{c_p} \boldsymbol{\nabla} \tilde{H}\right) + \overline{S_H} \tag{10}$$

where S_H is a volumetric source term that accounts for the heat transfer to the walls or due to thermal radiation, and k_t is the turbulent thermal conductivity, that in the case of the Standard *k-ε* turbulence model is usually given by

$$k_t = c_p\, \mu_t\, Pr_t^{-1} \tag{11}$$

where Pr_t is the turbulent Prandtl number, which by default is equal to 0.85 for two-equation RANS models.

For mixture fraction two additional transport equations are needed for solving its mean and variance values.

$$\boldsymbol{\nabla} \cdot \left(\overline{\rho}\, \tilde{\boldsymbol{u}}\, \tilde{Z}\right) = \boldsymbol{\nabla} \cdot \left(\frac{\mu + \mu_t}{Pr_t} \boldsymbol{\nabla} \tilde{Z}\right) \tag{12}$$

$$\boldsymbol{\nabla} \cdot \left(\overline{\rho}\, \tilde{\boldsymbol{u}}\, \widetilde{Z''^2}\right) = \boldsymbol{\nabla} \cdot \left(\frac{\mu + \mu_t}{Pr_t} \boldsymbol{\nabla} \widetilde{Z''^2}\right) + C_g\, \mu_t \left(\boldsymbol{\nabla} \tilde{Z}\right)^2 - C_d\, \overline{\rho} \frac{\tilde{\varepsilon}}{\tilde{k}} \widetilde{Z''^2} \tag{13}$$

where C_g and C_d are constants, equal to 2.86 and 2.0, respectively.

The mass production rates, $\dot{\omega}_k$, were solved according to GRI-Mech 3.0 chemical reaction mechanism, which consists of 325 elementary chemical reactions and contains 53 species, with variable thermodynamic and transport properties for each chemical species.

3.3 Radiation modeling

In this work, the heat source term, S_H, in the energy conservation equation accounts for heat transfer due to thermal radiation to the boundaries of the problem, thus being equal to the divergent of the radiative flux, $\boldsymbol{\nabla} \cdot \dot{q}_R''$. The gas absorption coefficient is modeled by the weighted-sum-of-gray-gases model (WSGGM). This model, introduced by Hottel and Sarofim (1967), replaces each participating gas by the sum of a small number of gray gases — CO_2 and H_2O in this case, which are usually suitable for combustion of hydrocarbon fuels (Coppalle and Vervisch, 1983) — resulting in the spectrum division in regions where the absorption coefficients can be considered constant.

The heat fluxes due to radiation were computed through the discrete transfer radiation model (DTRM). In this model, the change in radiant intensity of the i^{th} gray gas, I_i, is integrated over a path s for several directions through the radiative transfer equation (Denison and Webb, 1993), as follows

$$\frac{dI_i}{ds} = \kappa_i \left(a_i \frac{\sigma\, T^4\, s}{\pi} - I_i\, s\right) \tag{14}$$

where σ is the Stefan-Boltzmann constant, κ_i is the absorption coefficient of the i^{th} gray gas (Smith *et al.*, 1982), I_i is its spectral radiant intensity and a_i is its weighting factor (Coppalle and Vervisch, 1983).

Solved the radiative transfer equation, the source term for enthalpy due to radiation heat transfer is calculated locally by summing the changes in intensity for all the rays crossing the control volume, as

$$\overline{S_H} = \nabla \cdot \dot{q}_R'' = -\int_{\Omega=0}^{4\pi} \sum_i (\kappa_i I_i - \kappa_i a_i I_b)\, d\Omega \tag{15}$$

where Ω is the solid angle, I_b is the spectral radiant intensity correspondent to the emission of a black body.

3.4 Numerical methods and convergence criteria

The simulations were performed assisted by the commercial CFD code ANSYS Fluent, version 15.0.0, adopting second order for all spatial discretizations and the SIMPLE scheme for pressure-velocity coupling. The convergence criteria for all the computed properties were established for residuals lower than 1 10^{-8}, except for the radiative transfer equation, for which were adopted residuals lower than 1 10^{-4}.

4. MESH AND FLAMELET LIBRARY REFINEMENT EVALUATION

The study for results independence with respect to the mesh refinement level followed the guidelines from Celik *et al.* (2008). Four distinct meshes were adopted, with a minimum level of refinement, r, between them equal to 1.3, as recommended by the authors. The refinement factor between the meshes is expressed by

$$r = h_{coarser}/h_{finer} \tag{16}$$

where h corresponds to a representative average size of the mesh elements, defined by

$$h = \left(\frac{1}{n}\sum_{i=1}^{n} A_i\right)^{1/2} \tag{17}$$

where A_i is the area of each element in the mesh and n is its cells amount.

The geometrical domain comprises, longitudinally, 40 cm prior to fuel jet and air coflow exit and more 200 cm since it, and 40 cm, radially, as shown in Fig. 1, together with the boundary conditions.

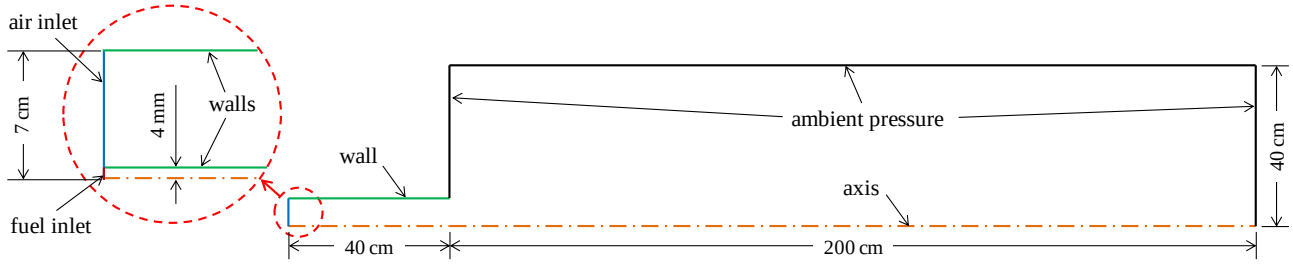

Figure 1. Geometrical domain and boundary conditions.

The two-dimensional meshes are composed by rectangular non-uniform size elements, with refinement concentrated at the region near the fuel jet. Automatic adaptation was applied to them, based on the gradient of the average mixture fraction field, starting with a primary grid, gradually refined while the iterations are running. For each mesh the mean values for longitudinal velocity, mixture fraction and temperature along the axis were obtained. The results are presented in Fig. 2. In this evaluation radiation modeling was not included.

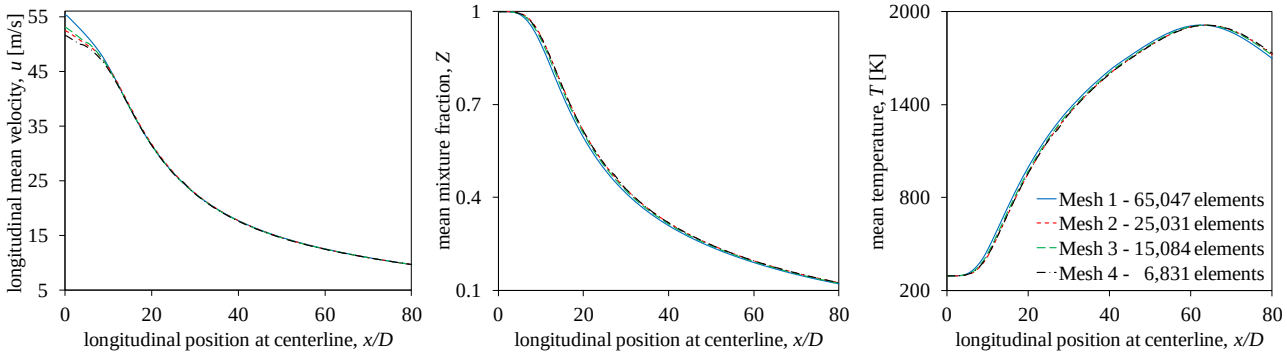

Figure 2. Dependence of the results according to mesh refinement level.

As can be seen in Fig. 2, except for longitudinal mean velocity near *x/D* = 0, the results for each mesh practically collapse. Thus, in this study was chosen the mesh nº 2, with 25,031 elements. It was also evaluated the refinement level of the databank generated to store the chemical properties from the flamelet solutions. Four databanks were generated, varying the amount of grid points for each controlling variable. The results dependence from the databank refinement level is practically undistinguishable. In this study was chosen the databank with 86 grid points in $\tilde{Z}$, 34 in $\widetilde{Z''^2}$, 130 in $\widetilde{\chi_{st}}$ and 35 in $\tilde{H}$ to carry the computations.

5. RESULTS AND DISCUSSION

The results for mean values are presented along the flow centerline. In the graphs are shown together the experimental measurements, the numerical results for the adiabatic solution and with radiation included, and the numerical results obtained by Pitsch (2000) and Lee and Choi (2009), when available.

Figure 3 shows the results for longitudinal mean velocity, mean mixture fraction and mean temperature. In general, the numerical results with radiation included are in better agreement to experimental measurements, especially for positions after *x/D* = 40 and for temperature prediction. The same behavior can be seen in the results obtained by Lee and Choi (2009) with and without radiation.

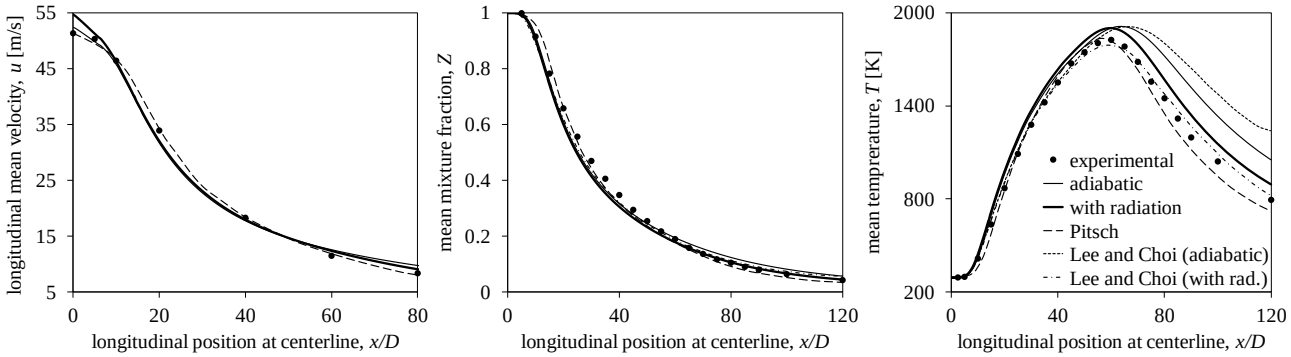

Figure 3. Results for longitudinal mean velocity, mean mixture fraction and mean temperature.

The improvement due to radiation is seen more clearly in the results for species mean mass fractions, in Fig. 4 and 5.

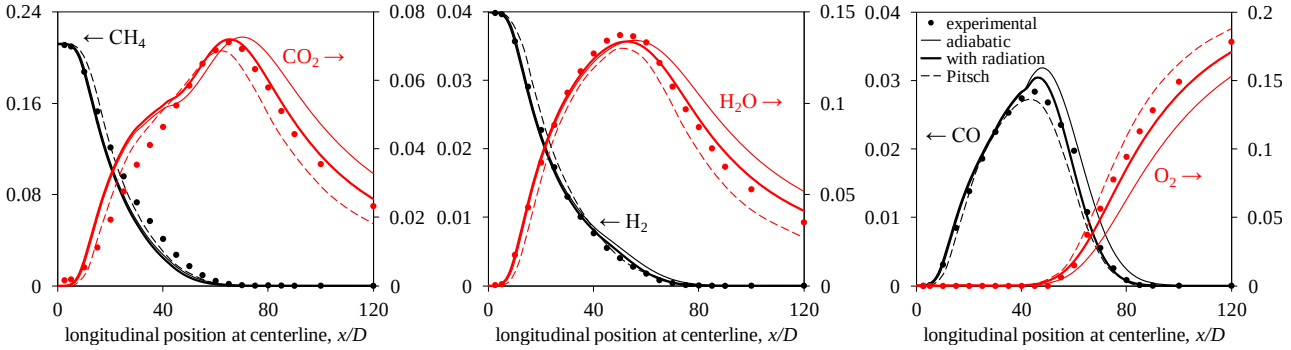

Figure 4. Results for mean mass fractions of species CH_4, CO_2, H_2, H_2O, CO and O_2.

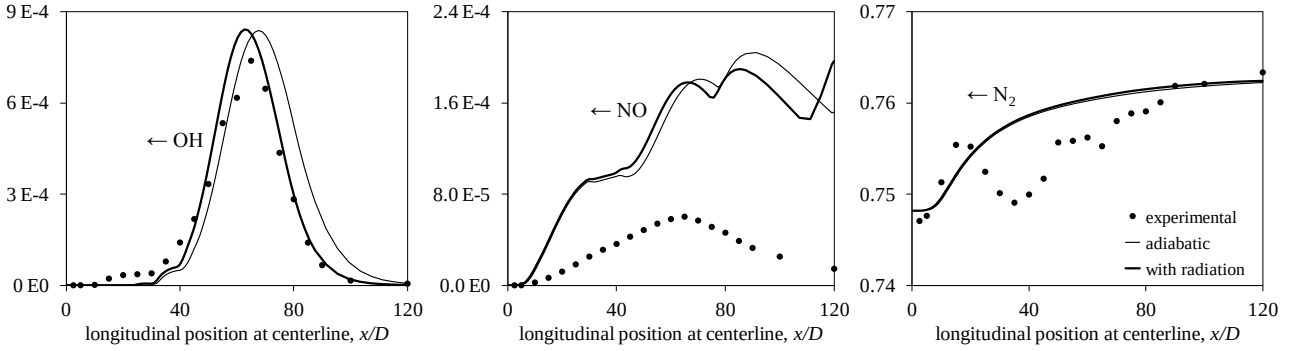

Figure 5. Results for mean mass fractions of species OH, NO and N_2.

The results improvement with inclusion of radiation for regions far from the fuel nozzle, after the peak of temperature, is assumed to be due to the strong dependence of temperature on radiation. The results for N_2, however, are barely the same with and without radiation. And, the results for NO, with or without radiation, are significantly far from the experimental measurements, what is assumed to be due to the deficiency of the steady laminar diffusion flamelet model in predicting the formation of species which involves slow reactions rates (Pitsch et al., 1998).

In this study the numerical results seem to be at least at the same level of agreement to experimental data than the ones obtained by Pitsch (2000). The author did not solve radiation, however, in his model the solution for unsteady flamelets is included, technique which is assumed to be more efficient in solving some slow-forming species, like NO_x (Coelho and Peters, 2001).

6. CONCLUSION

The present study investigated the performance of the steady laminar diffusion flamelet model for a non-premixed turbulent $CH_4/H_2/N_2$-air flame. Measured and predicted averaged values for longitudinal velocity, mixture fraction, temperature and species mass fractions showed to be in good agreement, and the inclusion of radiation improved the model accuracy, mainly for regions far from the fuel nozzle. The results for NO, however, with or without radiation, are significantly far from the experimental measurements, and it is expected that the inclusion of unsteady flamelets may improve its performance.

Thus, despite some discrepancies in the predicted quantities, the steady laminar diffusion flamelet model showed to be a useful tool in the numerical simulation for a turbulent reacting jet.

7. REFERENCES

Bergmann, V., Meier, W., Wolff, D. and Stricker, W., 1998. "Application of spontaneous Raman and Rayleigh scattering and 2D LIF for the characterization of a turbulent $CH_4/H_2/N_2$ jet diffusion flame". *Applied Physics B*, Vol. 66, pp. 489-502.

Bilger, R.W., 1988. "The structure of turbulent nonpremixed flames". In *Twenty-Second Symposium (International) on Combustion*, pp. 475-488.

Celik, I.B., Ghia, U., Roache, P.J., Freitas, C.J., Coleman, H. and Raad, P.E., 2008. "Procedure for estimation and reporting of uncertainty due to discretization in CFD application". *Journal of Fluids Engineering*, Vol. 130(7), p. 078001.

Coelho, P.J. and Peters, N., 2001. "Unsteady modelling of a piloted methane/air jet flame based on the Eulerian particle flamelet model". *Combustion and Flame*, Vol. 124(3), pp. 444–465.

Coppalle, A. and Vervisch, P., 1983. "The total emissivities of high-temperature flames". *Combustion and Flame*, Vol. 49(1-3), pp. 101-108.

Claramunt, A.K., 2005. *Numerical simulation of non-premixed laminar and turbulent flames by means of flamelet modelling approaches*. Ph.D. thesis, Universitat Politècnica de Catalunya, Catalonia.

Dally, B.B., Fletcher, D.F. and Masri, A.R., 1998. "Flow and mixing fields of turbulent bluff-body jets and flames". *Combustion Theory Modelling*, Vol. 2, pp. 193-219.

Denison, M.K. and Webb, B.W., 1993. "A spectral line-based weighted-sum-of-gray-gases model for arbitrary RTE solvers". *Journal of Heat Transfer*, Vol. 115(4), pp. 1004-1012.

Deon, D.L., Pereira, F.M., Hoerlle, C.A., Vielmo, H.A., 2014. "Comparison of turbulence models in RANS simulations of a nonreacting propane jet surrounded by coflowing air". In *15th Brazilian Congress of Thermal Sciences and Engineering*, Belém.

Emami, M.D. and Fard, A.E., 2012. "Laminar flamelet modeling of a turbulent $CH_4/H_2/N_2$ jet diffusion flame using artificial neural networks". *Applied Mathematical Modelling*, Vol. 36, pp. 2082–2093.

Hossain, M. and Malalasekera, W., 2005. "Numerical study of bluff-body flame structures using laminar flamelet model". In *Proceeding of the Institution of Mechanical Engineers*, Vol. 219, Part A: Journal of Power and Energy, pp. 361-370.

Hottel, H.C. and Sarofim, A.F., 1967. *Radiative Transfer*. McGraw-Hill, New York.

Janicka, J. and Kollmann, W., 1979. "A two-variables formalism for the treatment of chemical reactions in turbulent H_2-air diffusion flames". *Proceedings of the Combustion Institute*, Vol. 17, pp. 421–430.

Kim, J.S. and Williams, F.A., 1997. "Extinction of diffusion flames with nonunity Lewis number". *Journal of Engineering Mathematics*, Vol. 31(2), pp. 101-118.

Kim, S.H., Choi, C.H. and Huh, K.Y., 2005. "Second-order conditional moment closure modeling of a turbulent CH4/H2/N2 jet diffusion flame". *Proceedings of the Combustion Institute*, Vol. 30, pp. 735–742.

Klewer, C., 2011. *Numerische Berechnung von Verbrennungslärm und thermoakustischen Instabilitäten*. Doctorate thesis, Technisque Universität Darmstadt, Darmstadt.

Launder, B.E. and Spalding, D.B., 1972. *Lectures in Mathematical Models of Turbulence*. Academic Press, London.

Law, C.K., 2006. *Combustion Physics*. Cambridge University Press.

Lee, K.W. and Choi, D.H., 2009. "Analysis of NO formation in high temperature diluted air combustion in a coaxial jet flame using an unsteady flamelet model". *International Journal of Heat and Mass Transfer*, Vol. 52(5-6), pp. 1412–1420.

Lentini, D. and Puri, I.K., 1995. "Stretched laminar flamelet modeling of turbulent chloromethane-air nonpremixed jet flames". *Combustion and Flame*, Vol. 103(4), pp. 328–338.

Liu, F., Guo, H. and Smallwood, G.J., 2006. "Evaluation of the laminar diffusion flamelet model in the calculation of an axisymmetric coflow laminar ethylene-air diffusion flame". *Combustion and Flame*, Vol. 144, pp. 605-618.

Meier, W., Barlow, R.S., Chen Y.-L. and Chen, J.-Y., 2000. "Raman/Rayleigh/LIF measurements in a turbulent $CH_4/H_2/N_2$ jet diffusion flame: experimental techniques and turbulence–chemistry interaction". *Combustion and Flame*, Vol. 123, pp. 326-343.

Morse, A.P., 1977. *Axisymmetric turbulent shear flows with and without swirl*. Ph.D. thesis, London University, London.

Peters, N., 1984. "Laminar diffusion flamelet models in non-premixed turbulent combustion". *Progress in Energy and Combustion Science*, Vol. 10, pp. 319-339.

Peters, N., 1986. "Laminar flamelet concepts in turbulent combustion". In *Twenty-first Symposium (International) on Combustion/The Combustion Institute*, pp. 1231-1250.

Pitsch, H., 2000. "Unsteady flamelet modeling of differential diffusion in turbulent jet diffusion flames". *Combustion and Flame*, Vol. 123, pp. 358-374.

Pitsch, H., Chen, M. and Peters, N., 1998. "Unsteady flamelet modeling of turbulent hydrogen-air diffusion flames". In *Twenty-Seventh Symposium (International) on Combustion/The Combustion Institute*, pp. 1057–1064.

Pope, S.B., 1978. "An explanation of the turbulent round-jet/plane-jet anomaly". *AIAA Journal*, Vol. 16, Nº. 3, pp. 279-281.

Odedra, A. and Malalasekera, W., 2007. "Eulerian particle flamelet modeling of a bluff-body CH_4/H_2 flame", *Combustion and Flame*, Vol. 151(3) (2007), pp. 512–531.

Ravikanti, M., Hossain, M. and Malalasekera, W., 2009. "Laminar flamelet model prediction of NO formation in a turbulent bluff-body combustor". In *Proceeding of the Institution of Mechanical Engineers*, Vol. 223, Part A: Journal of Power and Energy, pp. 41-54.

Sanders, J.P.H., Chen, J.-Y. and Gökalp, I., 1997. "Flamelet based modeling of NO formation in turbulent hydrogen jet diffusion flames". *Combustion and Flame*, Vol. 111(1-2), pp. 1–15.

Sandia National Laboratories. "International workshop - measurements and computations of turbulent nonpremixed flames - $CH_4/H_2/N_2$ jet flames". <http://www.sandia.gov/TNF/DataArch/DLRflames.html>

Schneider, Ch., Dreizler, A., Janicka, J. and Hassel, E.P., 2003. "Flow field measurements of stable and locally extinguishing hydrocarbon-fuelled jet flames". *Combustion and Flame*, Vol. 135, pp. 185-190.

Smith, E.J., Mi, J., Nathan, G.J. and Dally, B.B., 2004. "Preliminary examination of a 'round jet initial condition anomaly' for the k-ε turbulence model". In *15th Australasian Fluid Mechanics Conference*, The University of Sydney, Sydney, pp. 13-17.

Smith, E.J., Nathan, G.J. and Dally, B.B., 2003. "Range of validity of a modified k-epsilon model of the non-reacting flow from a precessing jet nozzle". In *Third International Conference on CFD in the Minerals and Process Industries*, CSIRO, Melbourne, pp. 499-504.

Smith, T.F., Shen, Z.F. and Friedman, J.N., 1982. "Evaluation of coefficients for the weighted sum of gray gases model". *Journal of Heat Transfer*, Vol. 104(4), pp. 602-608.

TNF Workshop., 1998. *Proceedings of the Third International Workshop on Measurement and Computation of Turbulent Nonpremixed Flames*. Colorado.

Tabet-Helal, F., Sarh, B. and Gökalp, I., 2007. "Etude par simulation numérique des caractéristiques d'une flamme de diffusion turbulente avec co-courant d'air d'un mélange de CH_4-H_2". *Revue des Energies Renouvelables*, Vol. 10, N°. 2, pp. 173 – 180.

Wen, Z., Yun, S., Thomson, M.J. and Lightstone, M.F., 2003. "Modeling soot formation in turbulent kerosene/air jet diffusion flames". *Combustion and Flame*, Vol. 135(3), pp. 323–340.

Wilcox, D.C., 1998. *Turbulence Modeling for CFD*. DCW Industries, California, 2nd edition.

Yilmaz, D., Onbasioglu, S.U. and Gökalp, I., 2005. "Computational modeling of hydrogen enriched non-premixed turbulent methane air flames". In *Proceedings of European Combustion Meeting*, pp. 1-6.

Zakrzewski, W. and Ziólkowski, P., 2013. "Comparative study of turbulence modeling in methane simple jet flame". In *Colloquium Fluid Dynamics*, Institute of Thermomechanics AS CR, Prague, pp. 23-25.

Ziani, L., Chaker, A., Chetehouna, K., Malek, A. and Mahmah, B., 2013. "Numerical simulations of non-premixed turbulent combustion of CH_4-H_2 mixtures using the PDF approach". *International Journal of Hydrogen Energy*, Vol. 38, pp. 8597-8603.

8. RESPONSIBILITY NOTICE

The authors are the only responsible for the printed material included in this paper.